

Article

Synthesis and Catalytic Properties of Novel Ruthenacarboranes Based on *nido*-[5-Me-7,8-C₂B₉H₁₀]²⁻ and *nido*-[5,6-Me₂-7,8-C₂B₉H₉]²⁻ Dicarbollide Ligands

Ivan D. Grishin ^{1,*}, Anastasiya M. Zimina ¹, Sergey A. Anufriev ² , Nadezhda A. Knyazeva ¹, Alexander V. Piskunov ³ , Fedor M. Dolgushin ^{2,4}  and Igor B. Sivaev ^{2,5,*} 

- ¹ Department of Chemistry, Lobachevsky State University of Nizhny Novgorod, 23 Gagarin Prosp., 603950 Nizhny Novgorod, Russia; asya669pn@gmail.com (A.M.Z.); knyaseva2012@yandex.ru (N.A.K.)
² A.N. Nesmeyanov Institute of Organoelement Compounds, Russian Academy of Sciences, 28 Vavilov Str., 119991 Moscow, Russia; truman476@mail.ru (S.A.A.); fedya@xrlab.ineos.ac.ru (F.M.D.)
³ G.A. Razuvaev Institute of Organometallic Chemistry, Russian Academy of Sciences, 49 Tropinin Str., 603950 Nizhny Novgorod, Russia; pial@iomc.ras.ru
⁴ N.S. Kurnakov Institute of General and Inorganic Chemistry, Russian Academy of Sciences, 31 Leninskii Prosp., 119991 Moscow, Russia
⁵ Basic Department of Chemistry of Innovative Materials and Technologies, G.V. Plekhanov Russian University of Economics, 36 Stremyanniy Line, 117997 Moscow, Russia
* Correspondence: grishin_i@ichem.unn.ru (I.D.G.); sivaev@ineos.ac.ru (I.B.S.)



Citation: Grishin, I.D.; Zimina, A.M.; Anufriev, S.A.; Knyazeva, N.A.; Piskunov, A.V.; Dolgushin, F.M.; Sivaev, I.B. Synthesis and Catalytic Properties of Novel Ruthenacarboranes Based on *nido*-[5-Me-7,8-C₂B₉H₁₀]²⁻ and *nido*-[5,6-Me₂-7,8-C₂B₉H₉]²⁻ Dicarbollide Ligands. *Catalysts* **2021**, *11*, 1409. <https://doi.org/10.3390/catal11111409>

Academic Editors:
Annalisa Mariconda and
Pasquale Longo

Received: 30 October 2021
Accepted: 18 November 2021
Published: 21 November 2021

Publisher's Note: MDPI stays neutral with regard to jurisdictional claims in published maps and institutional affiliations.



Copyright: © 2021 by the authors. Licensee MDPI, Basel, Switzerland. This article is an open access article distributed under the terms and conditions of the Creative Commons Attribution (CC BY) license (<https://creativecommons.org/licenses/by/4.0/>).

Abstract: The effect of methyl substituents in the lower belt of dicarbollide ligands on the redox potential of ruthenacarboranes based thereof, as well as the ability of the metallocarboranes obtained to catalyze radical polymerization with atom transfer were studied. For this purpose, a new approach to the synthesis of *closo*-ruthenacarboranes based on substituted dicarbollide ligands was developed and six new complexes 3,3-(Ph₂P(CH₂)₄PPh₂)-3-H-3-Cl-9-Me-12-X-*closo*-3,1,2-RuC₂B₉H₉, 3,3,8-(Ph₂P(CH₂)₄PPh-μ-(C₆H₄-o))-3-Cl-9-Me-12-X-*closo*-3,1,2-RuC₂B₉H₈ and 3,3,4,8-(Ph₂P(CH₂)₄P-μ-(C₆H₄-o)₂)-3-Cl-9-Me-9-X-*closo*-3,1,2-RuC₂B₉H₇ (X = H, Me) were synthesized and characterized by single crystal X-ray diffraction, NMR and ESR spectroscopy and MALDI TOF mass-spectrometry. Comparison of the values of the redox potentials of the synthesized ruthenium complexes in 1,2-dichloroethane with the values previously found for the corresponding ruthenacarboranes based on the parent dicarbollide anion showed that the introduction of methyl substituents into the carborane cage led to a decrease in the redox potentials of the complexes, which made them more preferable catalysts for ATRP. Test experiments on the polymerization of MMA showed that the synthesized ruthenacarboranes were effective catalysts for ATRP, the most active being the complex with two methyl groups and two *ortho*-phenylenecycloboronated fragments.

Keywords: ruthenacarborane; synthesis; X-ray structure; electrochemistry; ATRP catalysis

1. Introduction

Metallocarborane clusters being the isolobal analogues of cyclopentadienyl derivatives of transition metals are of great interest due to their potential applications in catalysis. Metallocarborane-based catalytic systems were successfully used in selective carbene transfer reactions, photooxidation, dimerization of acetylenes and other processes including Atom Transfer Radical Polymerization (ATRP) [1–9]. According to the modern concept of ATRP, the catalytic performance of the complex significantly depends on its redox potential. A decrease in the oxidation potential leads to an increase in the activity of the catalyst and allows a decrease in its concentration while maintaining a high reaction rate [10,11].

Among the ways of decreasing the redox potential of metallocarboranes, the introduction of alkyl groups to the cage should be mentioned. According to Vinas and Teixidor, the introduction of one and two methyl groups to the carbon atoms of the carborane cage in

cobalt dicarbollide complexes leads to the gradual decrease of the redox potential [12]. The similar results were obtained in our group for the example of *closo*-ruthenarboranes with chelate diphosphine ligands. The introduction of methyl substituents to the carbon atoms of the dicarbollide ligand has a beneficial effect on reducing the oxidation potential [13], but increases steric hindrances due to the larger volume of methyl groups compared to hydrogen, which hampers the transfer of a halogen atom as a key step in the catalytic cycle.

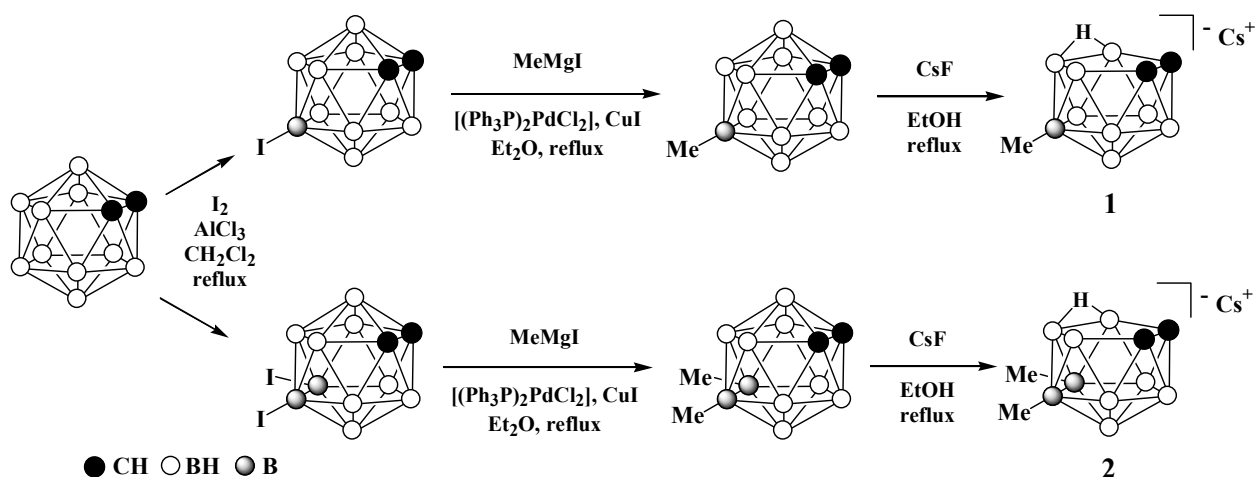
The contradictions between the electron-donating ability of alkyl substituents and the steric hindrances caused by them can be resolved by the substitution of hydrogen atoms in the lower belt of the dicarbollide cage. However, despite the fact that the synthesis of various *B*-alkyl derivatives of *ortho*-carborane is well documented [14], there are only a few examples of their use for the preparation of sandwiched or half-sandwiched metallocarboranes with alkyl substituents in the lower belt of the dicarbollide ligand [15,16].

In this contribution we report on the synthesis of novel *closo*-metallacarboranes on the base of the *B*-methylated dicarbollide ligands $[5\text{-Me-}7,8\text{-C}_2\text{B}_9\text{H}_{10}]^-$ and $[5,6\text{-Me}_2\text{-}7,8\text{-C}_2\text{B}_9\text{H}_9]^{2-}$, and study their reactivity and application in catalysis of polymerization of methyl methacrylate via the ATRP mechanism.

2. Results

2.1. Synthesis of *B*-Methylated *nido*-Carboranes

The cesium salts of the *B*-methylated *nido*-carboranes containing methyl groups in the lower belt of the carborane cage were prepared by Pd-catalyzed methylation of 9-iodo- and 9,12-diiodo-*ortho*-carboranes followed by deboronation of the resulting methylated *ortho*-carboranes upon treatment with cesium fluoride in refluxing ethanol (Scheme 1). The procedure was similar to the synthesis of the trimethylammonium salt of 5,6-dimethyl-*nido*-carborane [15], with the exception of using cesium fluoride instead of sodium hydroxide in the deboronation step. It should be noted that the synthesis of 5-methyl-*nido*-carborane by Pd-catalyzed methylation of 5-iodo-*nido*-carborane was reported earlier [17], however the purification procedure in this case was much more troublesome than in the case of methylation of 9-iodo-*ortho*-carborane.

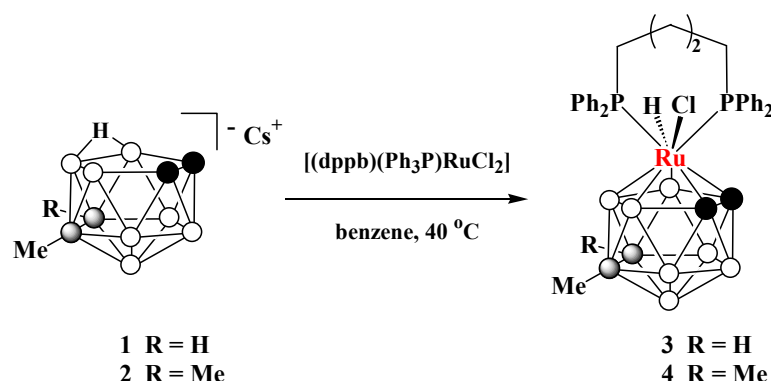


Scheme 1. Synthesis of *B*-methylated *nido*-carborane ligands.

2.2. Synthesis of *closo*-Ruthenaboranes

The conventional way to *closo*-ruthenacarboranes with chelate diphosphine ligands involves the use of the *exo-nido*-ruthenacarborane complexes as precursors, in which the ruthenium atom is coordinated to the *nido*-carborane cage via the B(5)H, B(6)H and B(10)H groups [18]. However, the presence of methyl substituents at the position B(5) of *nido*-carborane 1 and at the positions B(5) and B(6) of *nido*-carborane 2 makes the formation of such complexes impossible. Thus, we used the alternative route proposed

by Chizhevsky starting from the corresponding *nido*-carborane and $[(dppb)(Ph_3P)RuCl_2]$ (*dppb* is 1,4-bis(diphenylphosphino)butane) [19]. The reaction of *nido*-carboranes **1** and **2** with $[(dppb)(Ph_3P)RuCl_2]$ in benzene at 40 °C led to *closo*-ruthenacarboranes **3** and **4** as yellow-orange crystalline solids in 89 and 67% yields, respectively (Scheme 2).



Scheme 2. Synthesis of *closo*-ruthenacarboranes **3** and **4**.

The obtained diamagnetic complexes were characterized by NMR spectroscopy and single crystal X-ray diffraction. The ^{31}P NMR spectrum of **3** contains two multiplets at 38.0 and 36.3 ppm with integral ratio 1:1, while the ^{31}P NMR spectrum of **4** demonstrates one signal at 37.0 ppm (Figure 1). This may indicate the absence of free rotation of the dicarbollide ligand in the asymmetric complex **3**, which leads to the nonequivalence of two phosphorus atoms in the $Ph_2P(CH_2)_4PPh_2$ ligand. On the other hand, taking into account the equivalence of phosphorus atoms in complex **4**, it can be assumed that the diphosphine ligands in both complexes are located perpendicular to the plane passing through the B(3), B(8), and B(10) atoms of the dicarbollide ligand. It should be noted that the presence of methyl substituents in the dicarbollide ligand has no significant effect on the value of the ^{31}P chemical shift of the phosphine ligand as compared to those for the complex 3,3-($Ph_2P(CH_2)_4PPh_2$)-3-H-3-Cl-*closo*-3,1,2-Ru $C_2B_9H_{11}$ (**5**) based on the parent dicarbollide ligand (37.5 ppm) [18].

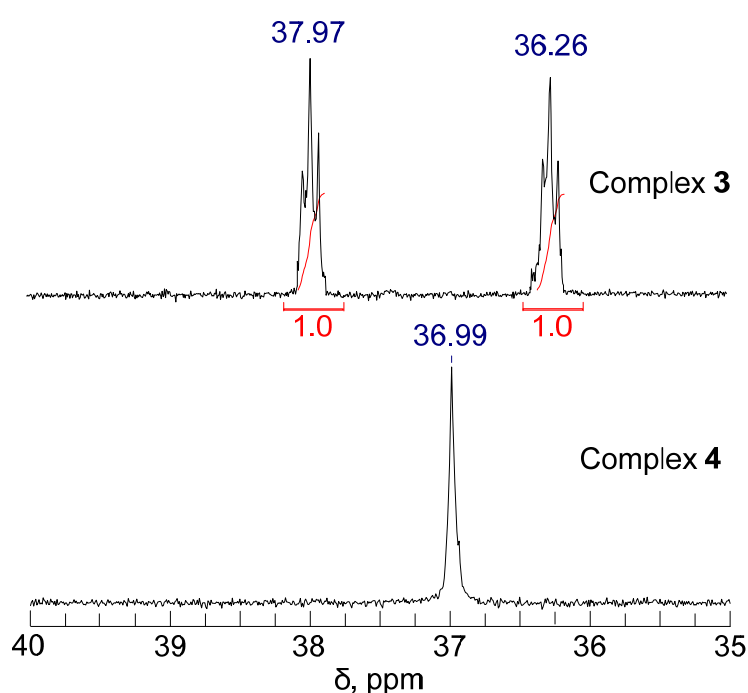
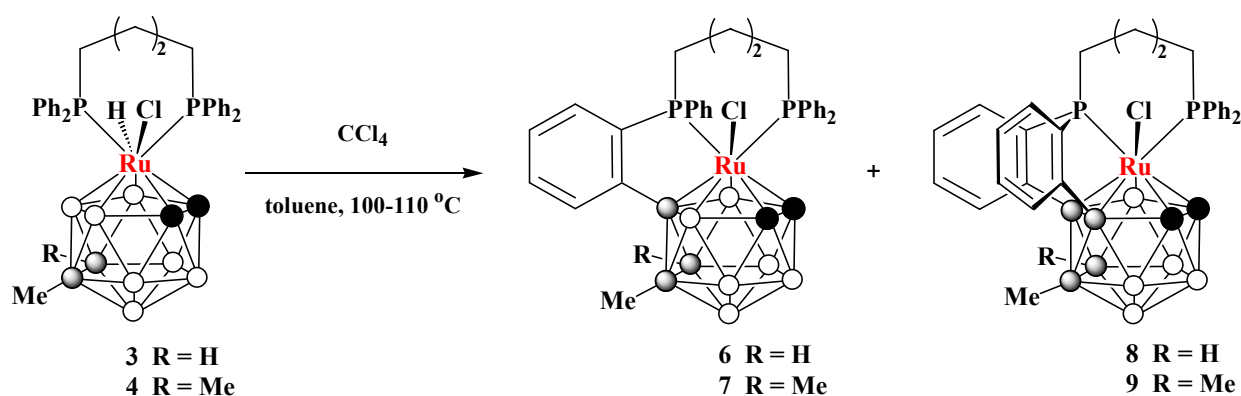


Figure 1. ^{31}P NMR spectra of complexes **3** and **4** in CD_2Cl_2 .

The ^1H NMR spectra of complexes **3** and **4** are typical for ruthenacarboranes with diphosphine ligands and contain signals from protons of aromatic rings and the polymethylene bridge in the ranges of 7.9–7.2 ppm and 3.6–1.5 ppm, respectively. The signals of methyl groups appear as singlets at ~ 0.05 ppm, while the signals of the Ru–H hydrides appear as multiplets approximately at -8.5 ppm. The signals of CH_{Carb} protons of **3** appear as two singlets at 3.62 and 2.88 ppm, while in the case of **4** the only signal at 3.23 ppm is observed, which is close to that observed for the complex **5** (3.28 ppm [18]). The 2D ^1H - ^{13}C HSQC, ^1H - ^1H COSY and ^1H NMR spectra of compounds **3** and **4** with the detailed signal assignment are provided in the Supplementary Information.

Heating of complexes **3** and **4** in toluene at 100°C followed by addition of 10-molar excess of carbon tetrachloride gives the 17-electronic paramagnetic complexes **6–9** as dark-red crystalline solids (Scheme 3). The introduction of the second methyl substituent into the carborane cage results in decrease of the complex stability leading to the lower yields as of the initial 18-electron complexes **3** and **4**, and so of its 17-electron derivatives **6–9**. The increase of the reaction temperature in the range 95 – 110°C results in higher yields of bis(*ortho*-cycloboronated) species **8** and **9** relative to its analogues **6** and **7** with one (*ortho*-cycloboronated) fragment.



Scheme 3. Synthesis of *closo*-ruthenacarboranes **6**, **8** and **7**, **9**.

The structures of complexes **6–9** were initially suggested based on the results of HPLC, MALDI MS, and EPR studies and finally confirmed by single crystal X-ray diffraction data. The mass-spectra contain envelope-type signals of the molecular anions typical for *closo*-ruthenacarboranes (see SI). The m/z values observed in the spectra of complexes **6** and **8** or **7** and **9** differ by 2 units in accordance with proposed formation of *ortho*-phenylenecycloboronated fragments. The presence of a covalent bond between the carborane and diphosphine ligands leads to an increase in the stability of the complexes under the conditions of the MALDI experiment, which leads to a decrease in the number of fragmentation signals in the mass spectra. Moreover, the mass spectra of compounds **6–9** do not contain signals from the free dicarbollide ligands, in contrast to the spectra of complexes **3–5**.

The paramagnetic nature of the complexes **6–9** was confirmed by EPR study. The spectra of complexes **6** and **8**, recorded in frozen toluene matrix, are shown in Figure 2, while similar spectra for **7** and **9** are provided in the Supplementary Information. The recorded spectra are typical for 17-electron paramagnetic ruthenacarboranes and exhibit rhombic g component patterns with $g_1 = 2386$, $g_2 = 2088$, $g_3 = 1966$ for **6**; $g_1 = 2380$, $g_2 = 2085$, $g_3 = 1968$ for **7**; $g_1 = 2316$, $g_2 = 2089$, $g_3 = 1978$ for **8**; $g_1 = 2312$, $g_2 = 2084$, and $g_3 = 1977$ for **9**. The spectra of complexes **6** and **7** are almost identical and have very close values of g -factors to each other and to the earlier described complex based on the parent *nido*- $\{\text{C}_2\text{B}_9\}$ carborane [3-Cl-3,3,8-[Ph₂P(CH₂)₄PPh- μ -(C₆H₄-*ortho*)]-*closo*-3,1,2-RuC₂B₉H₁₀] (**10**) with $g_1 = 2385$, $g_2 = 2095$, $g_3 = 1972$ [20]. The same is observed in the series **8**, **9** and [3-Cl-3,3,7,8-[Ph₂P(CH₂)₄P- μ -(C₆H₄-*ortho*)₂]-*closo*-3,1,2-RuC₂B₉H₉] (**11**) with two *ortho*-

cycloboronated fragments. The obtained values allowed us to suggest the presence of one and two *ortho*-cycloboronated fragments for compounds **6**, **7** and **8**, **9**, respectively. The mentioned coincidence of the spectra indicates that methyl substituents in the lower belt of the dicarbollide ligand are not involved in the delocalization of the unpaired electron and do not affect the conformation of the metal center.

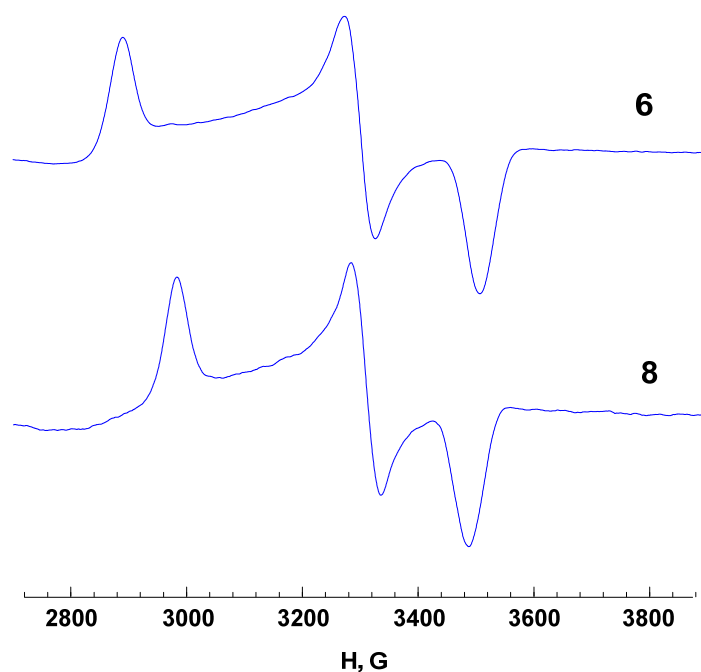


Figure 2. Anisotropic EPR spectra of ruthenacarboranes **6** and **8** in the toluene matrix at 77 K.

2.3. X-ray Diffraction Study of the Complexes

The suggested structures for complexes **3**, **4**, **7** and **9** were confirmed by single crystal X-ray diffraction study. The structure of complex **3** was earlier reported in our short communication [21], while the results of X-ray diffraction study of other complexes are presented in this work. The corresponding structures are given in Figure 3, Figure 4, Figure 5, while the most important bond lengths and angles are summarized in Table 1.

Complex **4** belongs to the group of neutral seven-coordinated Ru(IV) complexes. The ruthenium atom in **4** is quite symmetrically η^5 -coordinated by the dicarbollide ligand, so that the Ru-C and Ru-B distances between the metal center and atoms of the upper belt of the dicarbollide ligand are approximately equal. The general structural parameters of complexes should be noted that almost all are consistent with those in structurally similar complex **5** based on the parent dicarbollide ligand [20] and complex **3** with one methyl group in the cage. The presence of one and two methyl substituents at the B(9) and B(12) atoms results in a slight redistribution of bond lengths in the B(8)-B(9)-B(10)-B(12) fragment. The B(8)-B(9) bond length consecutive increases from 1.804(4) in **5** to 1.810(3) in **3** and 1.816(6) Å in **4** with the increase of steric hindrances. The configuration of the dppb ligand in **3** and **4** is similar to that in **5**. At the same time a slight decrease of the Ru-Cl bond is observed which can be attributed to the increase of electron density on the ruthenium atom, confirmed by cyclic voltammetry data discussed later.

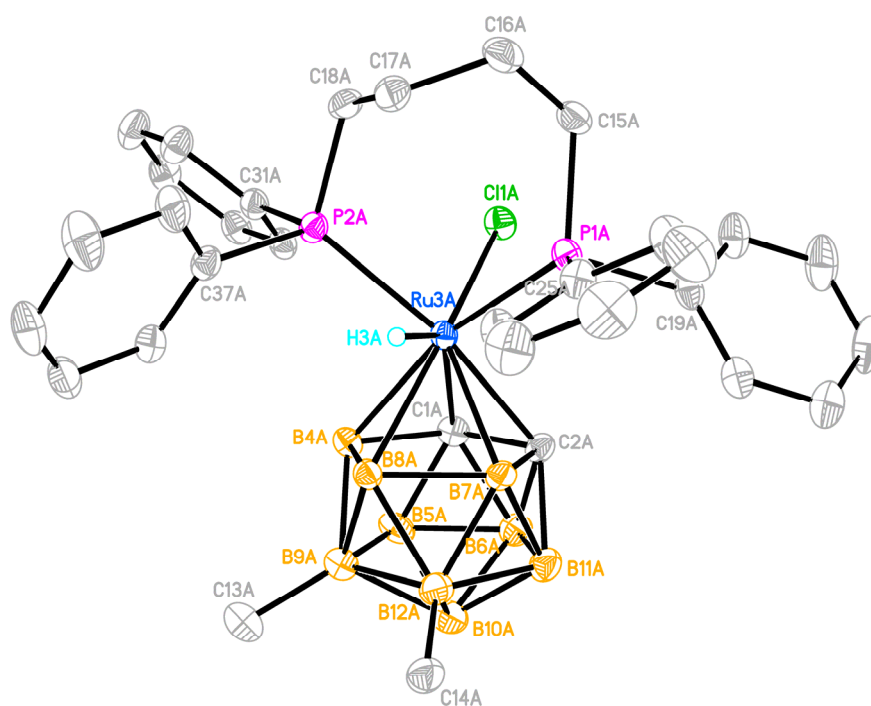


Figure 3. Molecular structure one of two symmetrically independent molecules of ruthenacarborane 4 (thermal ellipsoids drawn at the 50% probability level). Hydrogen atoms except the hydride ligand have been omitted for clarity.

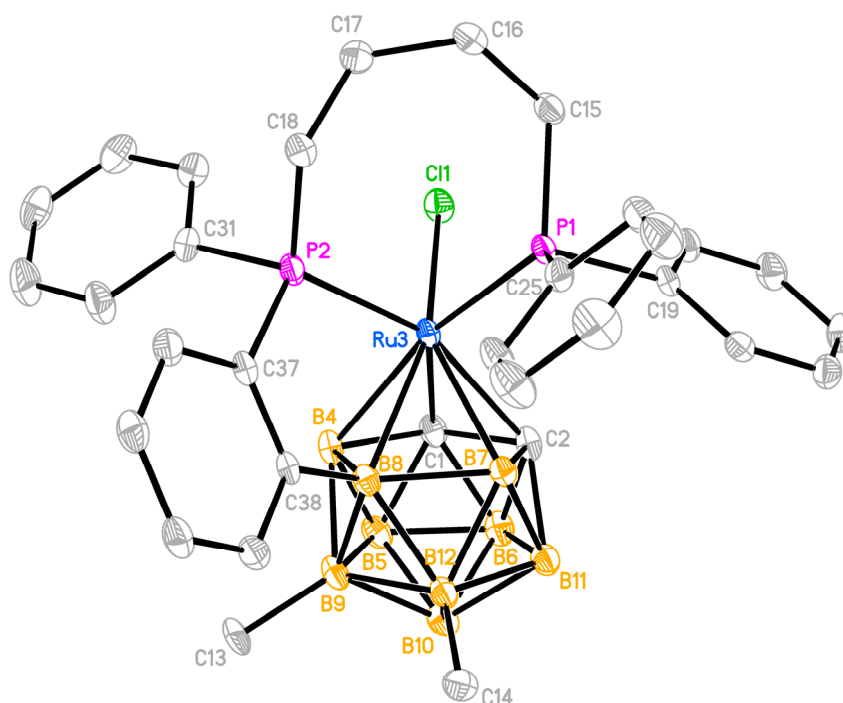


Figure 4. Molecular structure of ruthenacarborane 7 (thermal ellipsoids drawn at the 50% probability level). Hydrogen atoms have been omitted for clarity.

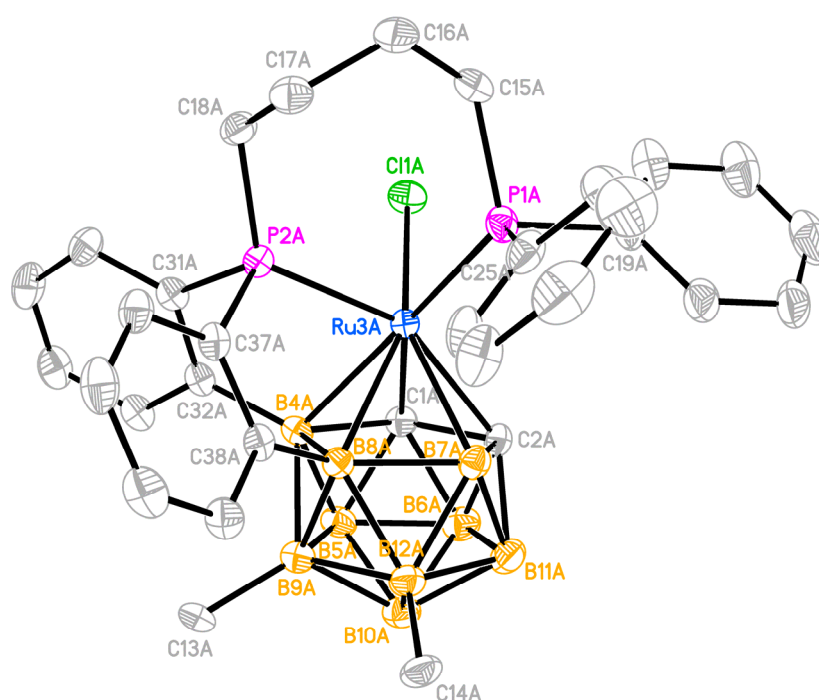


Figure 5. Molecular structure one of two symmetrically independent molecules of ruthenacarborane **9** (thermal ellipsoids drawn at the 50% probability level). Hydrogen atoms have been omitted for clarity.

Table 1. Selected bond lengths (Å) and angles (deg.) in the discussed ruthenacarboranes.

Parameter	Compound				
	5 [21]	3 [20]	4(A)	7	9(A)
	Bond lengths, Å				
Ru-P(1)	2.3670(5)	2.3701(6)	2.3620(8)	2.3688(8)	2.3509(9)
Ru-P(2)	2.3305(5)	2.3382(6)	2.3429(9)	2.2954(8)	2.2703(9)
Ru-H	1.51(3)	1.53(3)	1.50(4)		
Ru-Cl	2.4463(5)	2.4384(5)	2.4278(8)	2.3740(8)	2.3864(8)
Ru-C(1)	2.258(3)	2.220(2)	2.281(3)	2.240(3)	2.202(3)
Ru-C(2)	2.229(2)	2.198(2)	2.229(3)	2.256(3)	2.246(3)
Ru-B(4)	2.315(2)	2.296(2)	2.322(3)	2.251(3)	2.249(4)
Ru-B(7)	2.230(2)	2.265(2)	2.224(4)	2.232(3)	2.225(4)
Ru-B(8)	2.282(2)	2.298(2)	2.266(4)	2.291(3)	2.260(4)
C(1)-C(2)	1.624(3)	1.624(3)	1.624(3)	1.601(4)	1.617(5)
B(9)-B(12)	1.789(4)	1.798(4)	1.814(6)	1.800(5)	1.818(8)
B(8)-B(12)	1.805(3)	1.812(4)	1.818(5)	1.825(5)	1.825(7)
B(8)-B(9)	1.804(4)	1.810(3)	1.816(6)	1.836(5)	1.833(7)
B(10)-B(12)	1.782(4)	1.791(3)	1.798(6)	1.776(5)	1.801(9)
B(10)-B(9)	1.776(3)	1.783(4)	1.796(5)	1.776(5)	1.783(8)
B(8)-C(38)				1.587(4)	1.595(5)
B(4)-C(32)					1.586(5)
	Valence angles, deg.				
Cl-Ru-H	136(1)	136.40(1)	138.5(14)		
P-Ru-P	102.51(2)	102.28(2)	102.14(3)	90.11(3)	91.08(3)
P(1)-Ru-Cl	80.48(2)	80.48(2)	80.36(3)	90.24(3)	90.04(3)
P(2)-Ru-Cl	83.12(2)	83.16(2)	82.84(3)	95.68(3)	89.02(3)

The X-ray diffraction study of complexes **7** and **9** confirmed their 17-electron *closo*-structures being similar to those based on the parent dicarbollide ligand. The ruthenium

atom is bound in a η^5 -fashion to the C_2B_3 open face of the dicarbollide ligand and coordinated with a chlorine atom and two phosphorous of the dppb ligand. The Ru-P-Cl and P-Ru-P angles are close to 90° , being typical for 17-electron three-valent ruthenium in a pseudo-octahedral coordination state. The change of electron count at metal center from 18 in 3–5 to 17 in 7 and 9 has negligible effect on the Ru-C and Ru-B bonds, but results in a slight decrease (by 0.05 \AA) of the Ru-Cl bond. At the same time, the valence angles significantly differ. Among the peculiarities of complexes 7 and 9 the presence of one and two *ortho*-phenylenecycloboronated linkages between the dicarbollide and diphosphine ligands should be mentioned. The formation of the five-membered Ru-P-C-C-B-Ru cycle results in the decrease of the P(2)-Ru distance in 7 and 9 in comparison with complex 4. The observed values for the P-Ru-P and P-Ru-Cl angles, as well as for the Ru-P, Ru-Cl, Ru-C and Ru-B bonds in 7 and 9 are similar to those in earlier described ruthenacarboranes based on the parent dicarbollide ligand [20], indicating that introduction of methyl substituents in the lower belt of the dicarbollide ligand has no effect on the steric configuration of the metal center and should not create additional steric hindrances impeding catalytic applications.

2.4. Electrochemical Studies

Cyclic voltammetry studies were performed to study the effect of the methyl substituents in the dicarbollide ligand on the redox potentials of the ruthenacarboranes. The recorded CVA curves for novel ruthenacarboranes are provided in Figure 6. The electrochemical experiments were provided using an $\text{Ag} | \text{Ag}^+$ pseudo reference electrode, however the values of potentials were referred to ferrocene as the internal standard to provide more particular comparison with the earlier published results.

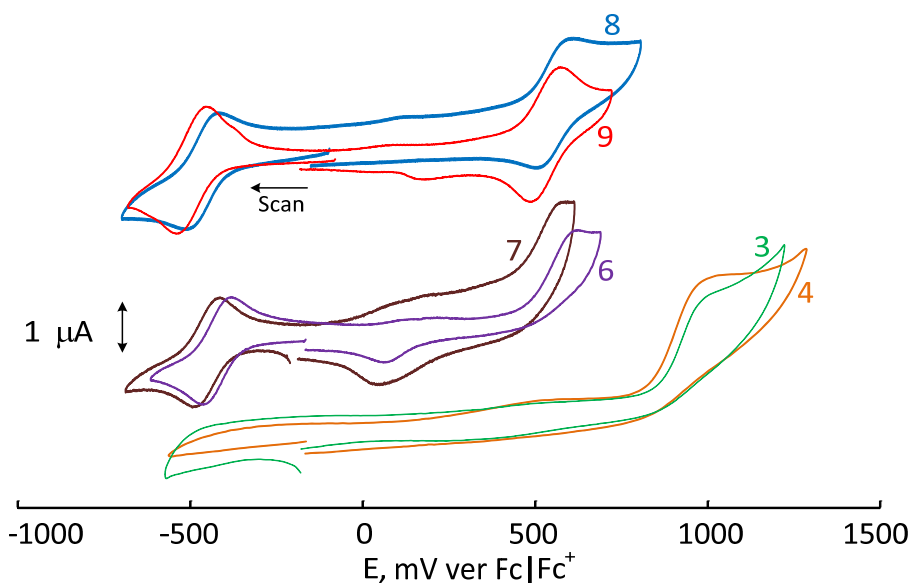


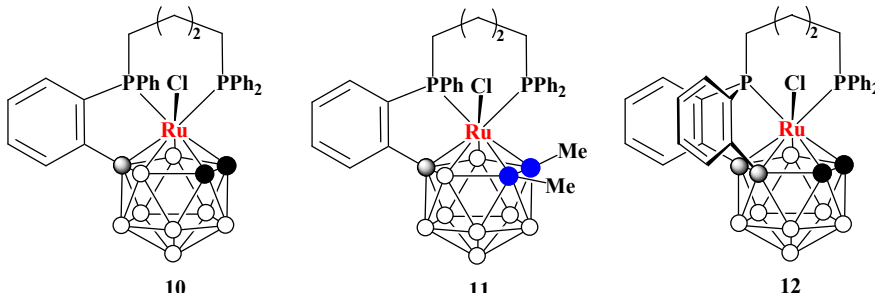
Figure 6. CVA curves for ruthenacarboranes in 1,2-dichloroethane ($C = 3 \times 10^{-3} \text{ M}$) at 25°C . Supporting electrolyte $n\text{-Bu}_4\text{NPF}_6$ (0.2 M). Scan rate 100 mV/s .

The Ru(IV) complexes 3 and 4 undergo irreversible oxidation at high potentials. At the same time, no reduction peak is observed in the studied range of potentials (down to -1700 mV versus $\text{Fc} | \text{Fc}^+$). The observed facts are in a good agreement with the high oxidative stability of such type of complexes, in spite of the presence of the hydride ligand. Complexes 3–5 may be stored at room temperature on air for a long time without noticeable decomposition. The introduction of the second methyl group in complex 4 results in a shift of the anodic peak to the area of lower potentials by 50 mV , which indicates the donor ability of the methyl substituent in the carborane cage, leading to an increase in the electron density at the metal center.

Ruthenacarboranes 6–9 formally contain Ru(III) and may be reduced to Ru(II) anions or oxidized to corresponding Ru(IV) species. The first process proceeds reversible in the case of all mentioned compounds, while the reversibility of oxidation is observed only for the complexes 8 and 9 containing two *ortho*-phenylenecycloboronated fragments. This observation is not surprising as it is in the full agreement with the behavior of the earlier explored complexes based on the parent dicarbollide ligand [13]. The possible explanation of this fact may be based on the earlier proposed mechanism of formation *ortho*-phenylenecycloboronated fragments as an electrophilic substitution in the phenyl ring of the diphosphine ligand [20]. One-electron oxidation of the complex results in the formation of an electrophilic center in the molecule. It is followed by intramolecular electrophilic substitution determining the irreversibility of oxidation of complexes 6 and 7. In the case of bis(*ortho*-cycloboronated) complexes 8 and 9 such reaction of the formed cation is impossible due to the existence of two covalent bonds between the carborane and diphosphine moieties.

Table 2 summarizes results of the electrochemical studies and the data on electrochemical behavior of earlier described *ortho*-cycloboronated derivatives 10, 12 and [3-Cl-3,3,8-(Ph₂P(CH₂)₄PPh-μ-(C₆H₄-*ortho*))-1,2-Me₂-*closo*-3,1,2-RuC₂B₉H₈] (11) [13]. According to the provided data the introduction of the methyl substituents in the dicarbollide ligand leads to the consecutive shift of the potential of the Ru(II) | Ru(III) transition into the lower values area making these complexes more perspective catalysts of controlled radical polymerization. The first substituent decreases the Ru(II) | Ru(III) redox potential approximately by 70 mV. The introduction of the second group leads to the further decrease of the potential, but the effect is lower—only about 30 mV. Such tendency is observed in the series of mono- and bis-(*ortho*-phenylenecycloboronated) complexes. At the same time, the effect of the methyl substituents on the Ru(III)-Ru(IV) transition is lower and is about 35 mV for the first and 25 for the second methyl group. The decrease of the contribution of the second substituent in the dicarbollide ligand on the global shift of the potential is similar to the observed behavior of sandwich pyrrolyl/dicarbollide cobalt complexes studied by Viñas and Teixidor [12].

Table 2. The results of electrochemical studies of the discussed ruthenacarboranes.



Transition	Compound									
	3	4	10 [13]	6	7	12 [13]	11 [13]	8	9	
M ⁻ / M	E_{pa} , mV	-	-	-316	-383	-417	-425	-358	-419	-454
	E_{pc} , mV	-	-	-393	-463	-487	-496	-428	-510	-540
	$E_{1/2}$, mV	-	-	-354	-423	-452	-461	-393	-464	-497
M / M ⁺	E_{pa} , mV	1010	960	683	600	576	554	627	601	571
	E_{pc} , mV	-	-	-	-	-	-	551	509	488
	$E_{1/2}$, mV	-	-	-	-	-	-	589	554	530

The comparison of the $E_{1/2}$ values for the mono- and bis(*ortho*-cycloboronated) species indicate that the latter are characterized by lower potentials. The formation of the *ortho*-phenylenecycloboronated fragment may be considered as the introduction of additional

substituent in the carborane cage. The comparison the $E_{1/2}$ values for $M^- | M^+$ transition for pairs 6 and 8, 7 and 9, 10 and 12 allows us to conclude that the presence of the second bond between the carborane and diphosphine moieties results in the decrease of the corresponding potential approximately by 40 mV. It should be noted that the measured $E_{1/2}$ value for Ru(II) | Ru(III) transition for complex 7 (-452 mV) is close to the same for its analogue 12 with two methyl groups bound to carbon atoms of the dicarbollide ligand ($E_{1/2} = -466$ mV). Thus, we may conclude that the electron donating effect of methyl substituent does not significantly depend on its position in the dicarbollide ligand.

2.5. Catalytic Activity in Radical Polymerization

The catalytic activity of ruthenacarboranes 6–9 in Atom Transfer Radical Polymerization was explored using methyl methacrylate (MMA) as a test monomer. The polymerization was initiated by carbon tetrachloride and conducted in accordance with AGET ATRP conception using isopropylamine as a reducing agent [22,23]. Toluene (25% vol.) was added to decrease viscosity of the reaction media and to improve the accuracy of the initiator dosage. The results of experiments on polymerization are summarized in Table 3 and Figures 7 and 8.

Table 3. The results of experiments on MMA polymerization in the presence of ruthenacarboranes 6–9 at 80 °C. [MMA]:[CCl₄]:[Ru]:[i-PrNH₂] = 10,000:25:1:40. Polymerization time—12 h.

Complex	Conversion	$M_n \times 10^{-3}$	M_w/M_n
6	66	28.6	1.38
7	56	21.2	1.38
8	62	30.7	1.47
9	94	39.2	1.34

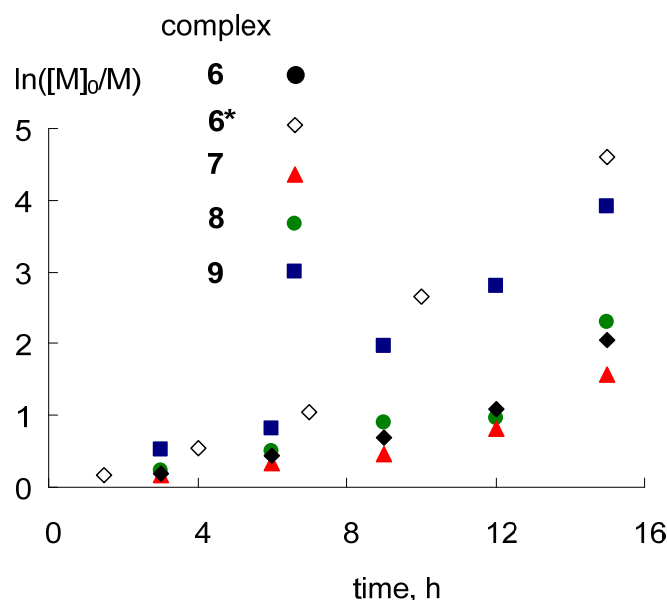


Figure 7. The dependences of $\ln[M]_0/[M]$ versus time for polymerization of MMA in the presence of ruthenacarboranes 6–9 at 80 °C. [MMA]:[CCl₄]:[Ru]:[i-PrNH₂] = 10,000:25:1:40. *—[MMA]:[CCl₄]:[Ru]:[i-PrNH₂] = 10,000:25:2:40.

Figure 7 illustrates kinetic plots for polymerization of MMA using novel ruthenium catalysts. It should be mentioned that such dependences are not linear and a slight induction period is observed at the initial stage of the process. This fact is in a good agreement with the proposed AGET ATRP mechanism. The catalyst is introduced into the system in the higher oxidation state as a deactivator. High concentration of the deactivator at the

initial stage leads to the shift of equilibrium in Scheme 4 to the dormant chains determining low polymerization rate. The gradual reduction of Ru(III) complex by isopropylamine results in the increase of Ru(II) activator concentration and consequential increase of the number of growing species and the polymerization rate. The increase of the catalyst concentration by two times has little impact on the initial polymerization rate, but results in significantly faster propagation of the process at higher conversion, as it was shown in the example of complex 6. This is also explained by accumulation of a reduced form of the catalyst at higher conversions.

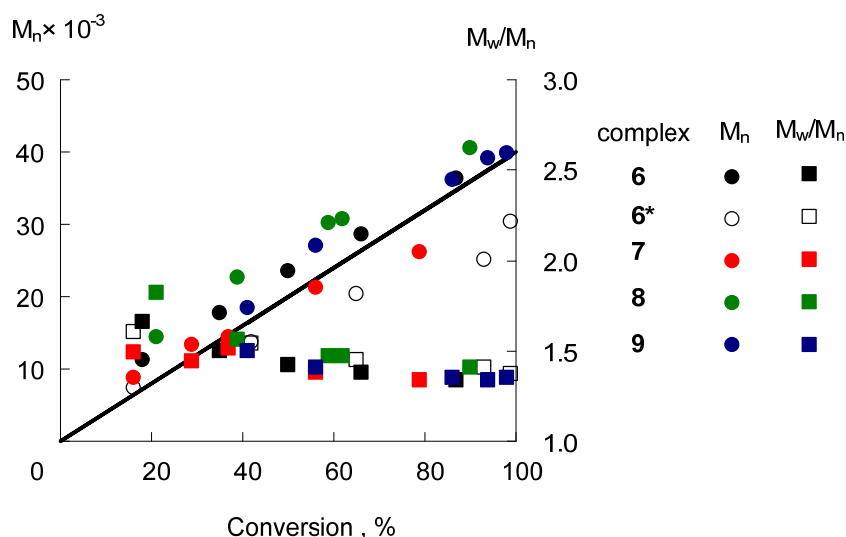
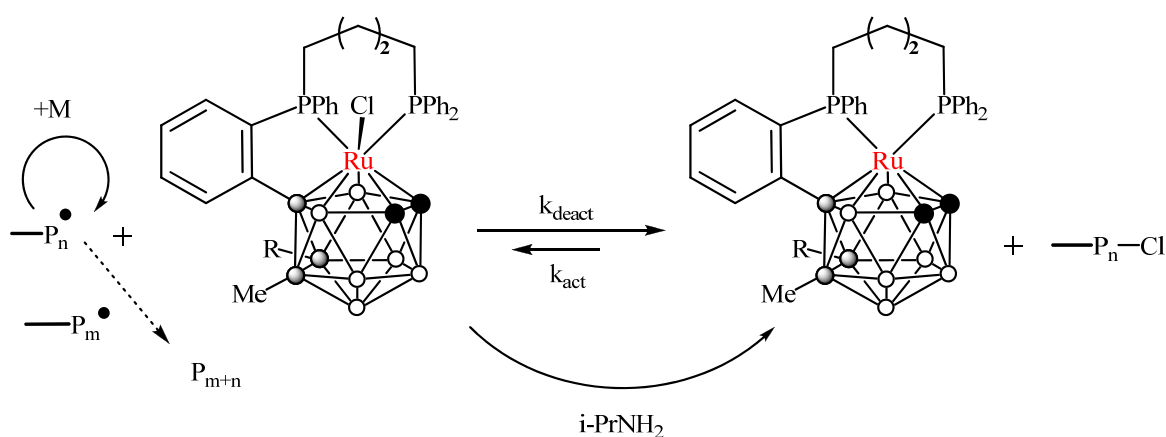


Figure 8. The dependences of number-average molecular weight (M_n) and dispersity (M_w/M_n) of MMA samples obtained in the presence of ruthenacarboranes 6–9 at 80 °C. [MMA]:[CCl₄]:[Ru]:[i-PrNH₂] = 10,000:25:1:40. *—[MMA]:[CCl₄]:[Ru]:[i-PrNH₂] = 10,000:25:2:40. Straight line—theoretically predicted values.



Scheme 4. The proposed AGET ATRP mechanism.

The comparison of the data obtained in the presence of different complexes allows us to conclude that the highest polymerization rate is observed in the presence of complex 9 with the lowest redox potential. The data provided in Figure 7 shows that the rate of the process catalyzed by 1 equivalent of 9 is almost the same as with two equivalents of 6. At the same time the increase of catalyst concentration results in the decay of the degree of control over the process. The obtained samples have lower molecular weights than theoretically calculated ones while the dispersity is higher than in the case of lower catalyst concentration.

The lowest dispersity (1.34) was observed for the samples obtained in the presence of complex **9** containing two methyl substituents and two *ortho*-cycloboronated fragments. The propagation of polymerization is accompanied by the linear increase of molecular weights with monomer conversion in good accordance with theoretically predicted values for all tested catalysts, while the best conformity is observed in the cases of **6** and **9**.

Thus, we may conclude that complex **9** seems to be the most preferable catalyst of ATRP among the tested ones. It allows obtaining well-defined polymers with a high rate even at low catalyst concentrations. The obtained results confirm the suggestion that the decrease of catalyst redox potential allows to improve the control over the process made by Matyjaszewski in the example on copper complexes [24]. Therefore, the obtained results are the bridge linking together the processes catalyzed by copper- and ruthenium-based complexes. The tuning metallocarborane catalyst of polymerization by the introduction of alkyl substituents in the lower belt of carborane cage may be considered as a way for its further modification. At the same time, the developed approach may be also applied to other catalytic processes catalyzed by metallocarboranes.

3. Experimental Part

3.1. Materials and Methods

9-Iodo-*ortho*-carborane [25], 9,12-diiodo-*ortho*-carborane [26], $[(\text{Ph}_3\text{P})_2\text{PdCl}_2]$ [27], $[(\text{dppb})(\text{Ph}_3\text{P})\text{RuCl}_2]$ [28], and complex **5** [20] were prepared according to the literature procedures. Diethyl ether, benzene and toluene were dried using standard procedures [29]. 1,4-Bis(diphenylphosphino)butane, cesium fluoride, and isopropylamine were purchased from DALCHEM (Nizhny Novgorod, Russia), P&M Invest (Moscow, Russia) and Sigma-Aldrich, respectively, and used without purification. All reactions were carried out at argon atmosphere. The reaction progress was monitored by thin layer chromatography (Merck F254 silica gel on aluminum plates) and visualized using 0.5% PdCl_2 in 1% HCl in aq. MeOH (1:10). Acros Organics silica 60 Å (0.060–0.200 mm) and Macherey-Nagel silica 60 Å (0.040–0.063 mm) were used for column chromatography of carboranes and metallocarboranes, respectively. The NMR spectra at 400 MHz (^1H) and 128 MHz (^{11}B) were recorded with Varian Inova 400 and Agilent DD2 NMR 400NB spectrometers. The residual signal of the NMR solvent relative to Me_4Si was taken as the internal reference for ^1H NMR spectra. ^{11}B NMR spectra were referenced using $\text{BF}_3 \cdot \text{Et}_2\text{O}$ as the external standard. The EPR spectra were recorded in frozen toluene at 77 K with a Bruker-EMX spectrometer, operating at 9.75 GHz. MALDI-TOF mass-spectra of complexes were obtained in a linear mode using a Bruker Microflex LT system and *trans*-2-[3-(4-*t*-butylphenyl)-2-methyl-2-propenylidene] malononitrile (DCTB) as a matrix. The solutions were applied to a stainless steel target plate and analyzed in positive and negative ion modes.

Electrochemical experiments were carried out by cyclic voltammetry (CV) in a three-electrode cell with platinum working and counter electrodes using an IPC Pro potentiostat. Tetrabutylammonium tetrafluoroborate was used as a supporting electrolyte; the potentials were measured relative to a silver pseudo-reference electrode (Ag wire in 0.1M AgNO_3 in MeCN). Ferrocene as the internal standard was introduced directly into the electrochemical cell after the recording CVA curve for the studied complex.

3.2. Preparation of Carborane Ligands

9-Methyl-*ortho*-carborane 9-Me-1,2- $\text{C}_2\text{B}_{10}\text{H}_{11}$ was prepared as described in the literature [30]. Methyl iodide (1.00 mL, 40% of the total amount) was added to a suspension of magnesium turnings (1.94 g, 80.00 mmol) in 50 mL of fresh distilled diethyl ether. The resulting mixture was heated under reflux until it became turbid. Then a solution of the remaining methyl iodide (1.50 mL, a total of 5.68 g, 40.00 mmol) in 50 mL of fresh distilled diethyl ether was added dropwise, and reaction was heated under reflux for another 1 h. After that, a solution of 9-iodo-*ortho*-carborane (2.70 g, 10.00 mmol) in 50 mL of fresh distilled diethyl ether was added dropwise, and the reaction was stirred at room temperature for another 1 h. Then bis(triphenylphosphine)palladium dichloride (0.35 g, 0.50 mmol,

catalytic amount) and copper iodide (0.10 g, 0.50 mmol, catalytic amount) were added. The reaction was heated under reflux for 40 h. Then the mixture was filtered and quenched with 50 mL of 5% aqueous solution of hydrochloric acid. The aqueous fraction was separated and extracted with diethyl ether (3 × 50 mL). The organic phases were combined, dried over Na₂SO₄ and concentrated under reduced pressure. The crude product was purified by column chromatography on silica with use of diethyl ether as the eluent to give a yellow solid of 9-methyl-*ortho*-carborane (1.49 g, yield 94%). ¹H NMR (400 MHz, CDCl₃): δ 3.49 (1H, br s, CH_{Carb}), 3.38 (1H, br s, CH_{Carb}), −0.24 (3H, s, BCH₃) ppm; ¹¹B NMR (128 MHz, CDCl₃): δ 7.5 (1B, s, B-C), −1.5 (1B, d, J = 149 Hz), −8.3 (2B, d, J = 149 Hz), −13.3 (2B, d, J = 145 Hz), −14.3 (2B, d, J = 135 Hz), −15.5 (2B, d, J = 164 Hz) ppm.

9,12-Dimethyl-*ortho*-carborane 9,12-Me₂-1,2-C₂B₁₀H₁₀ was prepared as described in the literature [26]. Methyl iodide (1.00 mL, 1/3 of the total amount) was added to a suspension of magnesium turnings (2.43 g, 100.00 mmol) in 50 mL of fresh distilled diethyl ether. The resulting mixture was heated under reflux until it became turbid. Then a solution of the remaining methyl iodide (2.11 mL, a total of 7.10 g, 50.00 mmol) in 50 mL of fresh distilled diethyl ether was added dropwise, and reaction was heated under reflux for another 1 h. After that solution of 9,12-diiodo-*ortho*-carborane (3.6 g, 10.00 mmol) in 50 mL of fresh distilled diethyl ether was added dropwise, and reaction was stirred at room temperature for another 1 h. Then bis(triphenylphosphine)palladium dichloride (0.70 g, 1.00 mmol, catalytic amount) and copper iodide (0.19 g, 1.00 mmol, catalytic amount) were added. The reaction was heated under reflux for 40 h. Then the mixture was filtered and quenched with 50 mL of 5% aqueous solution of hydrochloric acid. The aqueous fraction was separated and extracted with diethyl ether (3 × 50 mL). The organic phases were combined, dried over Na₂SO₄ and concentrated under reduced pressure. The crude product was purified by column chromatography on silica with use of diethyl ether as the eluent to give a yellow solid of 9,12-dimethyl-*ortho*-carborane (0.68 g, yield 40%). ¹H NMR (400 MHz, CDCl₃): δ 3.34 (2H, br s, CH_{Carb}), −0.20 (6H, s, BCH₃) ppm; ¹¹B NMR (128 MHz, CDCl₃): δ 7.4 (2B, s, B-C), −7.4 (2B, d, J = 147 Hz), −13.9 (4B, d, J = 162 Hz), −16.4 (2B, d, J = 177 Hz) ppm. The spectral data correspond to those described in the literature [14,25].

Cesium 5-methyl-7,8-dicarba-nido-undecaborate Cs[5-Me-7,8-C₂B₉H₁₁] (1). Cesium fluoride (1.52 g, 10.00 mmol) was added to a solution of 9-methyl-*ortho*-carborane (0.74 g, 4.70 mmol) in 25 mL of ethanol. The resulting mixture was heated under reflux for 24 h. After removal of volatiles under reduced pressure, the crude product was purified by column chromatography on silica with the use of a mixture of dichloromethane and acetonitrile (4:1, v/v) as the eluent to give a pale-yellow (0.66 g, yield 51%). ¹H NMR (400 MHz, acetone-d₆): δ 1.71 (1H, br s, CH_{Carb}), 1.46 (1H, br s, CH_{Carb}), −0.05 (3H, s, BCH₃), −2.80 (1H, s, BHB) ppm; ¹¹B NMR (128 MHz, CDCl₃): δ −4.8 (1B, s, B-C), −8.6 (1B, d, J = 137 Hz), −12.4 (1B, d, J = 135 Hz), −18.0 (1B, d, J = 167 Hz), −18.6 (1B, d, J = 131 Hz), −20.8 (1B, d, J = 147 Hz), −22.8 (1B, d, J = 145 Hz), −30.9 (1B, d, J = 134 Hz), −36.1 (1B, d, J = 140 Hz) ppm. The spectral data correspond to those described in the literature [17].

Cesium 5,6-dimethyl-7,8-dicarba-nido-undecaborate Cs[5,6-Me₂-7,8-C₂B₉H₁₀] (2). Cesium fluoride (1.52 g, 10.00 mmol) was added to a solution of 9,12-dimethyl-*ortho*-carborane (0.68 g, 4.00 mmol) in 25 mL of ethanol. The resulting mixture was heated under reflux for 24 h. After removal of volatiles under reduced pressure, the crude product was purified by column chromatography on silica with use of mixture of dichloromethane and acetonitrile (4:1, v/v) as the eluent to give a pale-yellow solid (0.88 g, yield 75%). ¹H NMR (400 MHz, acetone-d₆): δ 1.51 (2H, br s, CH_{Carb}), −0.04 (6H, s, BCH₃), −2.49 (1H, s, BHB) ppm; ¹¹B NMR (128 MHz, CDCl₃): δ −7.6 (2B, s, B-C), −9.9 (2B, d, J = 134 Hz), −18.6 (1B, d, J = 157 Hz), −21.3 (2B, d, J = 153 Hz), −28.9 (1B, d, J = 130 Hz), −34.2 (1B, d, J = 139 Hz) ppm. The spectral data correspond to those described in the literature [15].

3.3. Synthesis of Ruthenacarboranes

[3,3-(Ph₂P(CH₂)₄PPh₂)-3-Cl-3-H-9-Me-closo-3,1,2-RuC₂B₉H₁₀] (3). A mixture of [(dppb)(Ph₃P)RuCl₂] (106 mg, 0.123 mmol) and carborane 1 (140 mg, 0.142 mmol) was placed

in a Schlenk flask. The flask was degassed and filled with argon three times. After that 10 mL of benzene was added into the flask under argon flow and the reaction was stirred at 40 °C for 4 h. The solution was evaporated under reduced pressure and the residue was placed on a column filled with silica gel. A yellow-red band was eluted with an *n*-hexane-benzene (1:2) mixture. The evaporation of the obtained solution and recrystallization from benzene/*n*-hexane mixture gave 78 mg (89%) of complex **3** as yellow-orange crystals. Note: concentrated solutions of **3** have red color, while the diluted ones are orange or yellow. ¹H NMR (CD₂Cl₂, 400 MHz): δ 7.9-7.25 (20H, m, Ph-), 3.62 (1H, s, CH_{carb.}), 3.65 + 3.32 (1H + 1H, m, Ph₂PCH₂CH₂-), 2.88 (1H, s, CH_{carb.}), 2.60–2.45 (2H, m, Ph₂PCH₂CH₂-), 1.82+1.63 (3H+1H, m, Ph₂PCH₂CH₂-), 0.07 (3H, s, CH₃-B), –8.35 (1H, td, Ru-H) ppm. ³¹P NMR (CD₂Cl₂, 162 MHz): δ 38.0 (1P, m), 36.3 (1P, m) ppm. ¹¹B{¹H} NMR (CD₂Cl₂, 128 MHz): δ 8.7 (1B), 4.8(1B), –3.7 (1B), –2.4 (3B), –17.0 (1B), –19.2 (2B) ppm. MALDI MS (M[–], max): 709.3 ([M-H][–]; isotopic pattern for 1Ru, 1Cl, 9B atoms), calcd.: 709.2.

[3,3-(Ph₂P(CH₂)₄PPh₂)-3-Cl-3-H-9,12-Me₂-closo-3,1,2-RuC₂B₉H₉] (**4**). The procedure is similar as for the complex **3**. Starting from 93.3 mg (0.109 mmol) of [(dppb)(Ph₃P)RuCl₂] and 36.8 mg (0.125 mmol) of carborane **2**, 53 mg (67.3%) of **4** was obtained. ¹H NMR (CD₂Cl₂, 400 MHz): δ 7.9-7.25 (20H, m, Ph-), 3.43 (2H, m, Ph₂PCH₂CH₂-), 3.23 (2H, s, CH_{carb.}), 2.53 (2H, m, Ph₂PCH₂CH₂-), 1.82+1.57 (2H+2H, m, Ph₂PCH₂CH₂-), 0.04 (6H, s, CH₃-B), –8.47 (1H, td, Ru-H) ppm. ³¹P NMR (CD₂Cl₂, 162 MHz): δ 36.9 ppm. ¹¹B{¹H} NMR (CD₂Cl₂, 128 MHz): δ 9.7 (1B), 4.1 (2B), –2.2 (1B), –5.7 (2B), –17.2 (1B), –19.3 (2B). MALDI MS (M[–], max): 723.2 ([M-H][–]; isotopic pattern for 1Ru, 1Cl, 9B atoms), calcd.: 724.2.

[3,3,8-(Ph₂P(CH₂)PPh-μ-(C₆H₄-o)-3-Cl-9-Me-closo-3,1,2-RuC₂B₉H₉] (**6**) and [3,3,4,8-(Ph₂P(CH₂)₄P-μ-(C₆H₄-o)₂-3-Cl-9-Me-closo-3,1,2-RuC₂B₉H₈] (**8**). Complex **3** (134 mg, 0.189 mmol) was placed in a Schlenk flask and degassed via three vacuum–argon cycles and 20 mL of freshly distilled toluene were added. The reaction was carried under argon atmosphere at 100 °C with stirring for 5 h. After that, 0.3 mL of carbon tetrachloride was added and the flask was allowed to cool to room temperature. The solution was concentrated under vacuum and the residue was placed on a silica-gel filled column. The first dark red band was eluted by an *n*-hexane/benzene (1:2) mixture. The solution was evaporated, and residue was recrystallized from benzene/*n*-hexane to give 93.7 mg (70%) of complex **6**. Elution of the second red-brown band by pure benzene, followed by evaporation and recrystallization, gave 11.8 mg (9%) of complex **8**. Complex **6**: EPR (toluene, 77 K): g₁ = 2.386, g₂ = 2.088, g₃ = 1.966; MALDI MS (M[–], max): 707.3 (M[–]; isotopic pattern for 1Ru, 1Cl, 9B atoms), calcd.: 707.2. Complex **8**: EPR (toluene, 77 K): g₁ = 2.316, g₂ = 2.089, g₃ = 1.978; MALDI MS (M[–], max): 706.2 (M[–]; isotopic pattern for 1Ru, 1Cl, 9B atoms), calcd.: 706.2.

[3,3,8-(Ph₂P(CH₂)PPh-μ-(C₆H₄-o)-3-Cl-9,12-Me₂-closo-3,1,2-RuC₂B₉H₈] (**7**) and [3,3,4,8-(Ph₂P(CH₂)₄P-μ-(C₆H₄-o)₂-3-Cl-9,12-Me₂-closo-3,1,2-RuC₂B₉H₇] (**9**). The procedure is similar as for the complexes **6** and **8** described above. Heating complex **4** (81 mg, 0.112 mmol) in 20 mL of toluene at 110 °C for 5 h was followed by column chromatography separation; that gave 30 mg (37%) of **7** and 17 mg (21%) of **9**. Complex **7**: EPR (toluene, 77 K): g₁ = 2.380, g₂ = 2.085, g₃ = 1.968; MALDI MS (M[–], max): 722.2 (M[–]; isotopic pattern for 1Ru, 1Cl, 9B atoms), calcd.: 722.2. Complex **9**: EPR (toluene, 77 K): g₁ = 2.312, g₂ = 2.084, g₃ = 1.977; MALDI MS (M[–], max): 719.1 (M[–]; isotopic pattern for 1Ru, 1Cl, 9B atoms), calcd.: 719.2.

3.4. X-ray Diffraction Study

The X-ray single crystal data were collected using Mo K α radiation ($\lambda = 0.71073 \text{ \AA}$) on a Bruker D8Venture (Photon II detector, I μ S-microsource, focusing mirrors) diffractometer equipped with the Cryostream (Oxford Cryosystems, Long Hanborough, UK) open-flow nitrogen cryostats. All structures were solved by the direct method and refined by the full-matrix least squares technique against F^2 with anisotropic thermal parameters for all non-hydrogen atoms using the SHELXL software [31]. Hydrogen atoms of the dicarbollide ligands, as well as the hydride ligand in **4** were located from the Fourier syntheses and refined isotropically without restrictions. The other hydrogen atoms were placed geometri-

cally and included in the structure factors calculation in the riding motion approximation. Crystal data and parameters of the refinements are listed in Table 4. Crystallographic data for the structures were deposited with the Cambridge Crystallographic Data Centre as supplementary publications CCDC 2117788-2117790.

Table 4. The crystal data, data collection and structure refinement parameters for ruthenacarboranes 4, 7, 9.

Identification Code	4	7	9
CCDC No	2117788	2117789	2117790
Empirical formula	C ₃₂ H ₄₄ B ₉ ClP ₂ Ru	C ₃₂ H ₄₁ B ₉ ClP ₂ Ru	C ₃₂ H ₃₉ B ₉ ClP ₂ Ru CH ₂ Cl ₂
Molecular weight	724.42	721.40	804.31
Crystal size (mm)	0.16 × 0.10 × 0.06	0.22 × 0.16 × 0.02	0.16 × 0.12 × 0.04
Temperature (K)	150(2)	100(2)	100(2)
Crystal system	monoclinic	monoclinic	monoclinic
Space group	P2 ₁ /c	P2 ₁ /c	P2 ₁ /n
<i>a</i> (Å)	16.8803(10)	13.9369(18)	11.0895(3)
<i>b</i> (Å)	20.5774(12)	12.4716(16)	18.9868(5)
<i>c</i> (Å)	20.9312(12)	20.085(3)	34.9643(10)
β (deg)	106.242(2)	93.786(4)	90.0597(10)
<i>V</i> (Å ³)	6980.3(7)	3483.5(8)	7361.9(3)
<i>Z</i>	8	4	8
<i>D</i> _{calcd} (g·cm ⁻³)	1.379	1.376	1.451
linear absorption μ (cm ⁻¹)	6.41	6.42	7.56
<i>T</i> _{min} / <i>T</i> _{max}	0.904/0.963	0.913/0.987	0.898/0.970
2θ _{max} (deg)	56	60	56
Reflections collected	90,541	70,986	70,362
Independent reflections (<i>R</i> _{int})	16,854 (0.0878)	10,170 (0.0659)	17,778 (0.0618)
Observed reflections (<i>I</i> > 2σ(<i>I</i>))	11,813	8543	13,228
Number of parameters	900	440	938
<i>R</i> ₁ (on <i>F</i> for <i>I</i> > 2σ(<i>I</i>)) ^a	0.0419	0.0570	0.0474
<i>wR</i> ₂ (on <i>F</i> ² for all data) ^b	0.0918	0.0985	0.1088
<i>GOOF</i>	1.024	1.177	1.029
Largest diff. peak/hole (e Å ⁻³)	0.506/−0.710	1.257/−1.175	1.163/−1.081

$$^a R_1 = \sum ||F_o| - |F_c|| / \sum |F_o|; ^b wR_2 = \{\sum [w(F_o^2 - F_c^2)^2] / \sum w(F_o^2)\}^{1/2}$$

3.5. Polymerization Procedure

To avoid an error with a dosage of small initiator quantities, a 0.1 M CCl₄ solution in toluene was prepared. The predetermined amount of ruthenium complex (0.0047 mmol) was dissolved in 1.18 mL (0.118 mmol) of 0.1 M CCl₄ solution in a round-bottom flask. After full dissolution, 15.4 μL (0.188 mmol) of *i*-PrNH₂ and 5 mL (47 mmol) of MMA were added. The resulting mixture was poured out into five glass tubes (ca. 1.2 mL into each, the tubes were weighted before and after addition of the mixture) and the reaction mixture was degassed via three freeze-pump-thaw cycles to remove oxygen. The tubes were set to a thermostat for a certain time. The polymerization was stopped by freezing the tube with the reaction mixture by liquid nitrogen. The resulting polymer was precipitated into excess of *n*-hexane. In order to purify the polymers from residual amounts of the monomer, initiator, and the metallacarborane catalyst, the samples were twice dissolved in dichloromethane and precipitated into *n*-hexane. After the second precipitation, the samples were dried in vacuum to a constant weight. In the case of the use of a double amount of complex 6 as the catalyst, 0.0094 mmol of it was taken, while the quantities of other reagents were the same as described above.

Supplementary Materials: The following are available online at <https://www.mdpi.com/article/10.3390/catal11111409/s1>, Figures S1–S20: NMR spectra of compounds 1–4, Figures S21–S22: ESR spectra of compounds 7 and 9; Figures S23–S28: Mass-spectra of compounds 3, 4 and 6–9.

Author Contributions: Manuscript concept, electrochemical and MALDI MS experiments, supervision, and manuscript writing, I.D.G.; synthesis of metallocarboranes and HPLC experiments, A.M.Z.; synthesis and NMR spectroscopy of carborane ligands, S.A.A.; polymerization experiments, N.A.K.; EPR study, A.V.P.; single crystal X-ray diffraction experiments, and manuscript writing, F.M.D.; local supervision and manuscript writing, I.B.S. All authors have read and agreed to the published version of the manuscript.

Funding: This research was funded by the Russian Foundation for Basic Researches, grant number 20-33-90074. The EPR spectra were collected using the equipment of the Center for Collective Use of Scientific Equipment “Analytical Center of the G.A. Razuvaev Institute of Organometallic Chemistry” with the financial support of the grant “Ensuring the development of the material and technical infrastructure of the centers for collective use of scientific equipment” (Unique identifier RF-2296.61321X0017, Agreement Number 075-15-2021-670).

Data Availability Statement: Crystallographic data for the structures of compounds **4**, **7** and **9** were deposited with the Cambridge Crystallographic Data Centre as supplementary publications CCDC 2117788-2117790. The Supplementary Information contains NMR spectra of compounds **1–4**, ESR spectra of compounds **7** and **9** and mass-spectra of compounds **3**, **4** and **6–9**.

Acknowledgments: The NMR spectroscopy data of the carborane ligands were obtained by using equipment of the Center for Molecular Structure Studies at the A.N. Nesmeyanov Institute of Organoelement Compounds, operating with support from the Ministry of Science and Higher Education of the Russian Federation. The single crystal X-ray diffraction study was performed using shared experimental facilities of the N.S. Kurnakov Institute of General and Inorganic Chemistry supported by IGIC RAS state assignment.

Conflicts of Interest: The authors declare no conflict of interest. The funders had no role in the design of the study; in the collection, analyses, or interpretation of data; in the writing of the manuscript, or in the decision to publish the results.

References

1. Grimes, R.N. Carboranes in catalysis. In *Carboranes*, 3rd ed.; Academic Press: Cambridge, MA, USA, 2016; pp. 929–944. [CrossRef]
2. Gozzi, M.; Schwarze, B.; Hey-Hawkins, E. Half- and mixed-sandwich metallocarboranes in catalysis. In *Handbook of Boron Science with Applications in Organometallics, Catalysis, Materials and Medicine—Volume 2—Boron in Catalysis*; Hosmane, N.S., Eagling, R., Eds.; World Scientific Publishing Europe: London, UK, 2018; pp. 27–80. [CrossRef]
3. Zhu, Y.; Hosmane, N.S. Carborane-based catalysts for polymerization of olefins. In *Handbook of Boron Science with Applications in Organometallics, Catalysis, Materials and Medicine—Volume 2—Boron in Catalysis*; Hosmane, N.S., Eagling, R., Eds.; World Scientific Publishing Europe: London, UK, 2018; pp. 117–134. [CrossRef]
4. Tutusaus, O.; Delfosse, S.; Simal, F.; Demonceau, A.; Noels, A.F.; Núñez, R.; Viñas, C.; Teixidor, F. Half-sandwich ruthenium complexes for the controlled radical polymerisation of vinyl monomers. *Inorg. Chem. Commun.* **2002**, *5*, 941–945. [CrossRef]
5. Grishin, I.D.; Kolyakina, E.V.; Cheredilin, D.N.; Chizhevskii, I.T.; Grishin, D.F. Specifics of radical polymerization of styrene and methyl methacrylate in the presence of ruthenium carborane complexes. *Polym. Sci. A* **2007**, *49*, 1079–1085. [CrossRef]
6. Vinogradov, M.M.; Loginov, D.A. Rhoda- and iridacarborane halide complexes: Synthesis, structure and application in homogeneous catalysis. *J. Organomet. Chem.* **2020**, *910*, 121135. [CrossRef]
7. Guerrero, I.; Kelemen, Z.; Viñas, C.; Romero, I.; Teixidor, F. Photosensitizers for the photooxidation of alcohols in water through single-electron-transfer processes. *Chem. Eur. J.* **2020**, *26*, 5027–5036. [CrossRef] [PubMed]
8. Chan, A.P.Y.; Parkinson, J.A.; Rosair, G.M.; Welch, A.J. Bis(phosphine)hydridorhodacarborane derivatives of 1,1'-bis(orthocarborane) and their catalysis of alkene isomerization and the hydrosilylation of acetophenone. *Inorg. Chem.* **2020**, *59*, 2011–2023. [CrossRef] [PubMed]
9. Wang, L.; Perveen, S.; Ouyang, Y.; Zhang, S.; Jiao, J.; He, G.; Nie, Y.; Li, P. Well-defined, versatile and recyclable half-sandwich nickelacarborane catalyst for selective carbene-transfer reactions. *Chem. Eur. J.* **2021**, *27*, 5754–5760. [CrossRef] [PubMed]
10. Ribelli, T.G.; Fantin, M.; Daran, J.-C.; Augustine, K.F.; Poli, R.; Matyjaszewski, K. Synthesis and characterization of the most active copper atp catalyst based on tris[(4-dimethylaminopyridyl)methyl]amine. *J. Am. Chem. Soc.* **2018**, *140*, 1525–1534. [CrossRef]
11. Lorandi, F.; Matyjaszewski, K. Why do we need more active ATRP catalysts? *Isr. J. Chem.* **2019**, *60*, 108–123. [CrossRef]
12. Llop, J.; Viñas, C.; Teixidor, F.; Victori, L.; Kivekäs, R.; Sillanpää, R. Redox potential modulation in mixed sandwich pyrrolyl/dicarbollide complexes. *Inorg. Chem.* **2002**, *41*, 3347–3352. [CrossRef]
13. Grishin, I.D.; Turmina, E.S.; D'yachihin, D.I.; Peregudova, S.M.; Chizhevsky, I.T.; Grishin, D.F. Ruthenium carborane complexes: A relationship between the structure, electrochemical properties, and reactivity in catalysis of polymerization processes. *Russ. Chem. Bull.* **2013**, *62*, 692–698. [CrossRef]
14. Grimes, R.N. Icosahedral carboranes: 1,2-C₂B₁₀H₁₂. In *Carboranes*, 3rd ed.; Academic Press: Cambridge, MA, USA, 2016; pp. 283–502. [CrossRef]

15. Anufriev, S.A.; Sivaev, I.B.; Bregadze, V.I. Synthesis of 9,9',12,12'-substituted cobalt bis(dicarbollide) derivatives. *Russ. Chem. Bull.* **2015**, *64*, 712–717. [[CrossRef](#)]
16. Robertson, S.; Ellis, D.; Rosair, G.M.; Welch, A.J. Platination of $[3\text{-X-}7,8\text{-Ph}_2\text{-}7,8\text{-nido-C}_2\text{B}_9\text{H}_8]^{2-}$ (X = Et, F). Synthesis and characterisation of slipped and 1,2→1,7 isomerised products. *J. Organomet. Chem.* **2003**, *680*, 286–293. [[CrossRef](#)]
17. Zakharkin, L.I.; Ol'shevskaya, V.A.; Petrovskii, P.V. Synthesis of 5-organo-, 9-organo-, and 9,11-diorgano-nido-7,8-dicarbaundecaborane salts by cross-coupling. *Russ. J. Gen. Chem.* **2000**, *70*, 678–682.
18. Cheredilin, D.N.; Balagurova, E.V.; Godovikov, I.A.; Solodovnikov, S.P.; Chizhevsky, I.T. Facile formation of *exo-nido*→*closo*-rearrangement products upon the replacement of PPh₃ ligands with bis(diphenylphosphino)alkanes in “three-bridge” ruthenacarborane 5,6,10-[RuCl(PPh₃)₂]-5,6,10-(μ-H)₃-10-H-*exo-nido*-7,8-C₂B₉H₈. *Russ. Chem. Bull.* **2005**, *54*, 2535–2539. [[CrossRef](#)]
19. Grishin, I.D.; Turmina, E.S.; D'yachihin, D.I.; Vinogradov, D.S.; Piskunov, A.V.; Smolyakov, A.F.; Dolgushin, F.M.; Chizhevsky, I.T.; Grishin, D.F. Efficient catalytic systems based on paramagnetic *closo*-ruthenacarboranes for the controlled synthesis of polymers. *Russ. Chem. Bull.* **2011**, *60*, 2375–2383. [[CrossRef](#)]
20. Grishin, I.D.; D'yachihin, D.I.; Piskunov, A.V.; Dolgushin, F.M.; Smolyakov, A.F.; Il'in, M.M.; Davankov, V.A.; Chizhevsky, I.T.; Grishin, D.F. Carborane complexes of ruthenium(III): Studies on thermal reaction chemistry and the catalyst design for atom transfer radical polymerization of methyl methacrylate. *Inorg. Chem.* **2011**, *50*, 7574–7585. [[CrossRef](#)]
21. Zimina, A.M.; Anufriev, S.A.; Derendyaeva, M.A.; Knyazeva, N.A.; Somov, N.V.; Malysheva, Y.B.; Sivaev, I.B.; Grishin, I.D. Ruthenium complexes of 5-MeC₂B₉-carborane ligand: Synthesis and application in polymerization catalysis. *Doklady Chem.* **2021**, *498*, 97–103. [[CrossRef](#)]
22. Tang, H.; Radosz, M.; Shen, Y. CuBr₂/N,N,N',N'-tetra[(2-pyridyl)methyl] ethylenediamine/tertiary amine as a highly active and versatile catalyst for atom-transfer radical polymerization via activator generated by electron transfer. *Macromol. Rapid Commun.* **2006**, *27*, 1127–1131. [[CrossRef](#)]
23. Kwak, Y.; Matyjaszewski, K. ARGET ATRP of methyl methacrylate in the presence of nitrogen-based ligands as reducing agents. *Polym. Int.* **2009**, *58*, 242–247. [[CrossRef](#)]
24. Tang, W.; Kwak, Y.; Braunecker, W.; Tsarevsky, N.V.; Coote, M.L.; Matyjaszewski, K. Understanding atom transfer radical polymerization: Effect of ligand and initiator structures on the equilibrium constants. *J. Am. Chem. Soc.* **2008**, *130*, 10702–10713. [[CrossRef](#)]
25. Andrews, J.S.; Zayas, J.; Jones, M. 9-Iodo-*o*-carborane. *Inorg. Chem.* **1985**, *24*, 3715–3716. [[CrossRef](#)]
26. Zheng, Z.; Jiang, W.; Zinn, A.A.; Knobler, C.B.; Hawthorne, M.F. Facile electrophilic iodination of icosahedral carboranes. Synthesis of carborane derivatives with boron-carbon bonds via the palladium-catalyzed reaction of diiodocarboranes with Grignard reagents. *Inorg. Chem.* **1995**, *34*, 2095–2100. [[CrossRef](#)]
27. Itatani, H.; Bailar, J.C. Homogenous catalysis in the reactions of olefinic substances. V. Hydrogenation of soybean oil methyl ester with triphenylphosphine and triphenylarsine palladium catalysts. *J. Am. Oil Chem. Soc.* **1967**, *44*, 147–151. [[CrossRef](#)]
28. Jung, C.W.; Garrou, P.E.; Hoffman, P.R.; Caulton, K.G. Reexamination of the reactions of Ph₂P(CH₂)_nPPh₂ (n = 1–4) with RuCl₂(PPh₃)₃. *Inorg. Chem.* **1984**, *23*, 726–729. [[CrossRef](#)]
29. Armarego, W.L.F.; Chai, C.L.L. *Purification of Laboratory Chemicals*, 6th ed.; Butterworth-Heinemann: Burlington, NJ, USA, 2009.
30. Gal'chenko, G.L.; Tamm, N.B.; Pavlovich, V.K.; Ol'shevskaya, V.A.; Zakharkin, L.I. 9-Methyl-*o*-carbaborane(12). Synthesis and determination of thermochemical characteristics. *Organomet. Chem. USSR* **1990**, *3*, 203–206.
31. Sheldrick, G.M. Crystal structure refinement with SHELXL. *Acta Cryst. C* **2015**, *71*, 3–8. [[CrossRef](#)]